Comparison of Experiment and the Proposed General Linear Viscoelastic Theory. 4. Concentrated Polymer Solution Systems

Y.-H. Lin

Baytown Polymers Center, Exxon Chemical Company, Baytown, Texas 77522.
Received July 10, 1986

ABSTRACT: Concentrated polymer solutions are prepared from blending a nearly monodisperse low molecular weight (MW) polystyrene (as the solvent, $M_w = 10\,300 < M_e$, the entanglement MW) with a series of nearly monodisperse polystyrenes with MW much greater than M_e. The systems are perfect for testing the proposed general linear viscoelastic theory in the concentrated solution regime. The linear viscoelastic relaxation spectrum line shapes of the studied samples are analyzed in terms of a combination of the Rouse theory (for the low-MW component as the solvent) and the general theory (for the high-MW component as the polymer). It is shown that the entanglement MW (M_e') in the solution scales as $M_e' = M_e W_H^{-1}$ for polystyrene, where W_H is the weight fraction of the high-MW component. The universality of the proposed theory is as applicable in the concentrated solutions as in the pure melts. Very significantly, we have found that, within experimental errors, the friction coefficients in the Rouse part and in the part of the general theory are identical as extracted from the spectrum line shape analysis. As with some previous results reported in paper 3, this strongly supports that the proposed general theory has bridged the gap between the Rouse theory and the Doi–Edwards theory.

I. Introduction

A general linear viscoelastic theory[1] (paper 1) for monodisperse flexible linear polymer melts and concentrated solutions has been developed based on the Doi–Edwards theory[2-5] and the chain contour length fluctuation effect similar to those proposed by Doi.[6,7] The linear viscoelastic relaxation spectra of a wide range of (nearly) monodisperse polystyrene samples of different molecular weight (MW) have been measured and their line shapes have been well-analyzed quantitatively in terms of the proposed theory[8,9] (papers 2 and 3). The analysis has explained why and how the modulus plateau of the linear viscoelastic relaxation gradually diminishes with decreasing MW and explained the MW dependence of the zero-shear viscosity ($\eta_0 \propto M^{3.4}$ for $M > M_C$ and $\eta_0 \propto M$ for $M < M_C$) and the steady-state compliance, J_e. The constraint effect due to entanglement as described by the proposed theory persists to MW as low as $\sim 1.2M_e$. Further, the pure reptational times calculated from the linear viscoelasticity and diffusion motion data in terms of the theory are in good agreement.[10] The validity of the proposed general linear viscoelastic theory is, thus, extensively and consistently supported by the experimental results.

It has been shown in the line shape analysis of linear viscoelastic spectra that the Rouse theory is applicable just below M_e, while the general linear viscoelastic theory is applicable above M_e.[8,9] The transition point, M_e, appears quite sharp. At M_e, the zero-shear viscosity value of the Doi–Edwards theory is greater than the Rouse value by a factor of 2.4. The general theory has bridged the gap to about 30% of difference (η_0 calculated with $K'/K = 1$ in the general theory).[9] The 30% difference should be due to the topological constraint effect imposed on the polymer chain at M_e.

In this report, we study polymer blend systems consisting of two monodisperse polystyrene components: one having a MW just below M_e, while the other a MW far above M_e. In such systems, the entanglement density associated with the high-MW component is diluted by the low-MW component. On the other hand, the low-MW component is still free of entanglement and maintains its Rouse dynamic behavior. Such binary blends provide systems equivalent to concentrated polymer solutions. The solvent (the low-MW component) has the identical chemical structure as the polymer (the high-MW component). The studied systems, with the solvent MW being still quite high ($M_L > M_H^{0.5}$, where M_H is the MW of the high-MW component[11]) and being in the concentrated region, should remain in the Θ condition at different temperatures. In other words, the chain configuration of the high-MW component is Gaussian in the solutions as in its pure melt state. On the one hand, such concentrated solution systems are ideal for testing the universality of the proposed general linear viscoelastic theory. On the other hand, they represent a special case of binary blend systems. The study of such systems can provide us detailed information for developing a more complete picture of the molecular mechanism for the blending law.

II. Theory

Four dynamic modes have been identified in the polymer linear viscoelastic behavior: the Rouse chain motion between two cross-linked points (or fixed entanglement points), $\mu_A(t)$; the chain slippage through entanglement links, $\mu_X(t)$; the primitive chain length fluctuation, $\mu_B(t)$; and the reptational motion corrected for the chain length fluctuation effect, $\mu_C(t)$. Including all the four dynamic modes, a general functional form for the stress relaxation modulus following a step shear deformation in the linear regime has been obtained for a monodisperse system. For the polymer blends of two monodisperse components (with W_L and W_H being weight fractions for the low- and high-MW components, respectively), in which the low MW (M_L) is slightly smaller than M_e, while the high MW (M_H) is much greater than M_e, the theoretical form for the stress relaxation modulus can be written as (see the Appendix)

$$G(t) = W_L \frac{\rho RT}{M_L} \mu_R(t/\tau_R) + W_H \frac{4\rho RT}{5M_e'} [1 + \mu_A(t/\tau_A)] \times [1 + (1/4)\exp(-t/\tau_X)][B\mu_B(t/\tau_B) + C\mu_C(t/\tau_C)] \quad (1)$$

where

$$\mu_R(t/\tau_R) = \sum_{p=1}^{N_R-1} \exp(-t/\tau_R^p) \quad (2)$$

with

$$\tau_R^p = \frac{K\pi^2}{24 \sin^2(\pi p/2N_R)} \frac{M_L^2}{N_R^2} \quad (3)$$

$$\mu_A(t/\tau_A) = \sum_{p=1}^{N_e'-1} \exp(-t/\tau_A^p) \quad (4)$$

with

0024-9297/87/2220-0885$01.50/0

$$\tau_A{}^p = \frac{K\pi^2}{24 \sin^2 (\pi p/2N_e')} \frac{M_e'^2}{N_e'^2} \quad (5)$$

$$B = (M_e'/M)^{1/2} \quad (6)$$

$$C = 1 - B \quad (7)$$

$$\mu_B(t/\tau_B) = \sum_{p\,\mathrm{odd}} \frac{8}{\pi^2 p^2} \exp(-p^2 t/\tau_B) \quad (8)$$

with

$$\tau_B = (1/3)KM^2 \quad (9)$$

and

$$\mu_C(t/\tau_C) = \sum_{p\,\mathrm{odd}} \frac{8}{\pi^2 p^2} \exp(-p^2 t/\tau_C) \quad (10)$$

with

$$\tau_C = K\frac{M^3}{M_e'} [1 - (M_e'/M)^{1/2}]^2 \quad (11)$$

All the notations are the same as in the previous reports, except M_e' is the entanglement MW of the solution, which has N_e' Kuhn segments, and N_R is the number of the Kuhn segments associated with the low-MW chain (A Rouse chain).

All the relaxtion times in the above equations are proportional to the constant K given as

$$K = \frac{\zeta b^2 N_0{}^2}{kT\pi^2 M^2} \quad (12)$$

where ζ, b, and M/N_0 are the friction constant, length, and mass associated with each Kuhn segment, respectively. For easy reference in comparing the K values extracted from the line shape analysis of the linear viscoelastic spectra below, the K constants of eq 3 and 5 are designated as K'' and K', respectively.

M_e' can be determined from the plateau modulus G_N of the pure melt and the volume fraction (equivalent to weight fraction in the present case) of the high-MW component and as shown in the Appendix is given as

$$M_e' = \frac{4\rho RT}{5G_N W_H} = \frac{M_e}{W_H} \quad (13)$$

where M_e is the entanglement MW in the melt state of the pure monodisperse component. The plateau modulus, G_N', of the solution can be defined as

$$G_N' = \frac{4\rho RT W_H{}^2}{5M_e} \quad (14)$$

Both the static quantities, B and C, are expressed in terms of the reduced MW: M/M_e'. As we normalize τ_B and τ_C with respect to $\tau_A{}^1$, all the relaxation times are functions of the reduced MW as well. Thus, the theoretical form of stress relaxation for the entangled component is universal in terms of the reduced MW.

By keeping the universality applicable in the $\mu_X(t)$ region, we have obtained through a combination of a scaling argument and analysis of the experimental results of the monodisperse melts

$$\tau_X = 0.55KM_e'M \quad (15)$$

where M_e has been substituted by M_e' (see papers 1 and 2).

G_N, M_e, and MWD have all been extracted from the line shape analysis of the linear viscoelastic relaxtion spectra of the studied monodisperse samples,[8,9] and W_L and W_H are predetermined in preparing the solutions. The linear viscoelastic relaxation spectrum line shapes of the solutions can be calculated from all these known quantities. In the comparison with the measured linear viscoelastic relaxation line shapes over the entire time or frequency domain, the values of the ratios K'/K and K''/K are the only adjustable parameters. From analyzing the linear viscoelastic relaxation line shapes of the monodisperse melts, it was shown that K'/K has a plateau value of about 3.3 (after a 30% correction due to the width of MWD) in the high-MW region and decreases to a limiting value of 1 with decreasing MW. We will show below that the K'/K values of the concentrated solutions follow the same universal curve, when MW is normalized with respect to M_e or M_e'.

III. Experiment

The concentrated solutions consisting of a low-MW component (F1, M_w = 10 300) and a high-MW component X (X = P7, M_w = 68 000; F10, M_w = 100 000; F35, M_w = 355 000; F80, M_w = 775 000) have been prepared at the percentage ratios of P7/F1 = 50/50 and 75/25, F10/F1 = 50/50 and 75/25, F35/F1 = 50/50, and F80/F1 = 50/50. F1, F10, F35, and F80 were obtained from Toyo Soda Manufacturing Co., Japan. F35 is their later version of F40. To avoid confusion with the F40 sample (M_w = 422 000) used previously, the new sample is labeled F35 here. P7 was obtained from Polysciences, Inc. The details of the linear viscoelastic relaxation measurements and preparation of samples are as described before.[1,8,9]

IV. Line Shape Analysis of Linear Viscoelastic Relaxation Spectra

The $G(t)$ or $G'(\omega)$ and $G''(\omega)$ spectra of the studied X/F1 blend samples (X = P7, F10, F35, and F80) are calculated by convoluting eq 1 (in combination with eq 2–11, 13, and 15) with the *same MWDs* that have been used to calculate the linear viscoelastic spectra fitting to the measured results of the F1 sample and the X components in the pure melt state. The MWD of F1 is that used in paper 3 (Z = 120 for the Schulz MWD). The MWDs of P7 (Z = 120) and F10 (Z = 60) have been shown in Figure 16 of paper 2.[8] The three-component MWDs of F35 and F80 have been obtained from the nonlinear least-squares fitting to the $G(t)$ curves of their pure melt samples in the terminal region as described previously.[1,8] Their M_w/M_n values are 1.13 and 1.24 for F35 and F80, respectively. These M_w/M_n values of F35 and F80 are somewhat higher than their GPC values. This has been explained as due to the intrinsic broader MWD and low-MW components (a low-MW tail in the GPC spectrum) in these samples.[1,8] The linear additivity of contributions from separate MW components assumed in the $G(t)$ line shape analysis is not strictly obeyed. As explained in paper 2, this is generally so at high MWs. As a result, the parameters K and K'/K obtained from the $G(t)$ line shape analysis at high MWs have certain systematic errors, which depend on the width of the MWD. The errors associated with the studied samples are small and their magnitudes have been estimated.

Because of dilution, the M_e' (or N_e') value of the solution is increased according to eq 13. The M_e value of the monodisperse polystyrene melt has been determined from its plateau modulus to be 13 500 at 127.5 ± 0.5 °C. The corresponding N_e value has been assumed to be 10, which is sufficiently large for the data analysis in the $\mu_A(t)$ process region, as explained previously.[1,8]

Since the M_e' and the MWD of the monodisperse components in the X/F1 blend samples have been predetermined, the only adjustable parameters in the line shape analysis of the linear viscoelastic spectra are the K'/K and K''/K values. For MW > M_e, K'/K has been shown greater than 1 in the monodisperse melts. Its physical

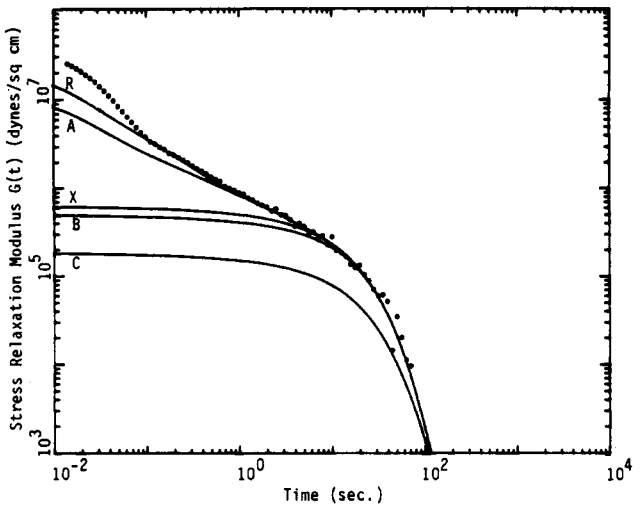

Figure 1. Comparison of the measured (···) and calculated (—) stress relaxation moduli, $G(t)$, for the P7/F1 = 50/50 sample. Also shown are the separate contributions of the $\mu_R(t)$ process of F1 and the $\mu_A(t)$, $\mu_X(t)$, $\mu_B(t)$, and $\mu_C(t)$ processes of P7. $K'/K = 1.4$, $K''/K = 1$, $M_e' = 27\,000$, $N_e' = 20$, and $N_R = 8$ are used in the calculation.

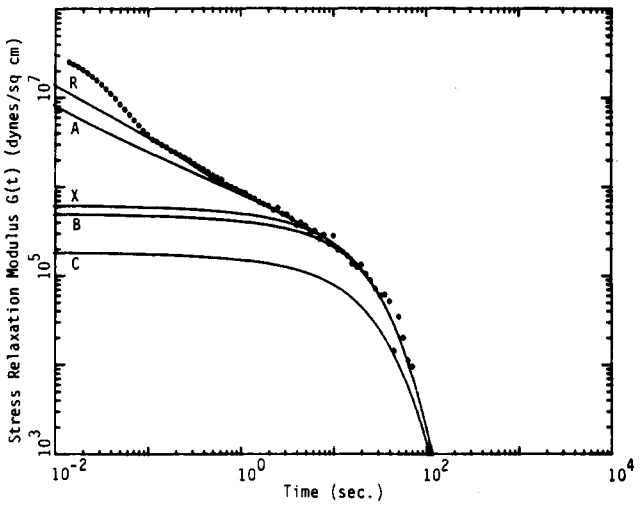

Figure 2. Same as Figure 1 except that $N_e' = 40$ and $N_R = 16$ are used in the calculation.

meaning has been explained in paper 2.

The measured and calculated $G(t)$ curves of the P7/F1 = 50/50 sample are shown in Figure 1. $K'/K = 1.4$, $K''/K = 1$, $M_e' = 27\,000$, $N_e' = 20$, and $N_R = 8$ (equivalent to $N_e = 10$) have been used in the calculation. The contributions of the Rouse process, $\mu_R(t)$ of the F1 component and the $\mu_A(t)$, $\mu_X(t)$, $\mu_B(t)$, and $\mu_C(t)$ processes of P7, are shown in the figure as labeled. Since $\tau_A > \tau_R$, the experimental curve and the theoretical curve calculated without the contribution from the $\mu_R(t)$ process are first matched to determine the K'/K value. The difference in the shorter time region is then matched by including the $\mu_R(t)$ process to determine the K''/K value. The glassy relaxation process begins to contribute in the time region of the fast relaxation modes of $\mu_R(t)$. The glassy relaxation process is not included in the analysis. Matching the lowest few modes of $\mu_R(t)$ to the experimental curve is sufficient to determine the K''/K value. For the other X/F1 blend samples, the same procedure is followed in the line shape analysis as shown below. In the comparison of theory and experiment, all the measured curves are shifted to superpose on the calculated curves using $K = 1 \times 10^{-8}$.

To show that the K'/K and K''/K values obtained this way are independent of the chosen N_e' and N_R values as

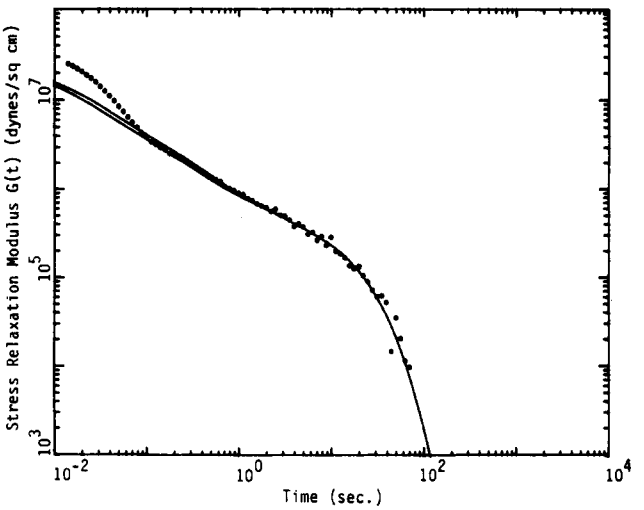

Figure 3. Comparison of the measured $G(t)$ values with the theoretical curves (—) calculated with $K''/K = 1$ and $K''/K = 1.5$ for the P7/F1 = 50/50 example. The rest is the same as in Figure 1.

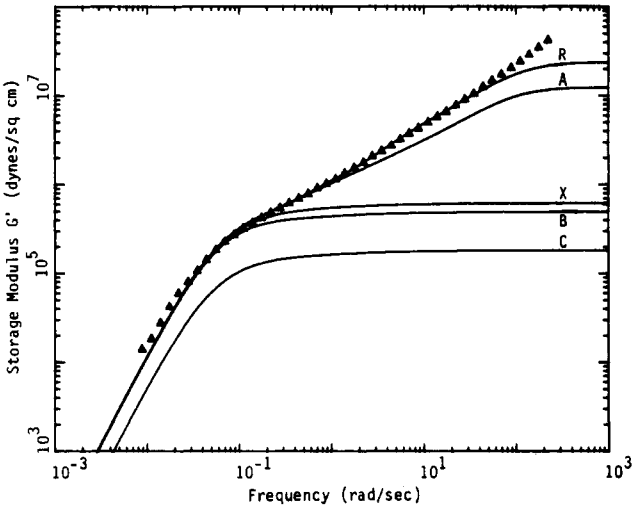

Figure 4. Comparison of the measured (▲) and calculated (—) storage moduli, $G'(\omega)$, for P7/F1 = 50/50. The parameters used in the calculation are the same as in Figure 1. Also shown are the separate contributions of the $\mu_R(t)$ process of F1 and the $\mu_A(t)$, $\mu_X(t)$, $\mu_B(t)$, and $\mu_C(t)$ processes of P7.

long as they are sufficiently large, the theoretical curve is also calculated with $N_e' = 40$ and $N_R = 16$ (i.e., doubling the number of segments per unit mass) and compared with the measured one for P7/F1 = 50/50 as shown in Figure 2. It is clear from comparing Figures 1 and 2 that the change of the N_e' and N_R values only affects the $G(t)$ curve in the short-time region, where the glassy relaxation is important. In the time region of our interest, the choice of the N_e' and N_R values has no effect on the K'/K and K''/K values obtained from the line shape analysis as long as they are sufficiently large. $N_e = 10$ used in the previous reports is a reasonable value, and its corresponding N_e' and N_R values are used in all the line shape calculations below.

In Figure 3, we show the comparison of the theoretical curves of $K''/K = 1$ and $K''/K = 1.5$ together with the measured values for P7/F1 = 50/50. This comparison indicates the sensitivity of the calculated curve to the variation of the K''/K value and the possible error of the obtained K''/K value from comparing with the experimental results. It is fair to say that the possible error of $K''/K = 1$ is about 20% according to Figure 3.

To confirm the $G(t)$ line shape analysis of the P7/F1 = 50/50 sample, the calculated and measured $G'(\omega)$ and

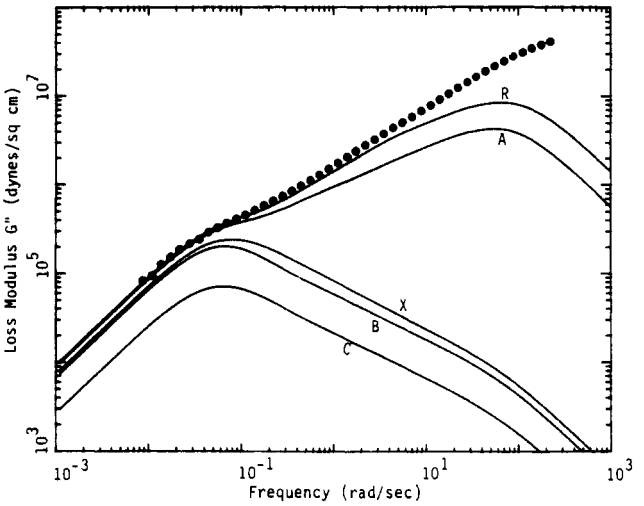

Figure 5. Same as in Figure 4 for the loss moduli, $G''(\omega)$, measured (●) and calculated (—).

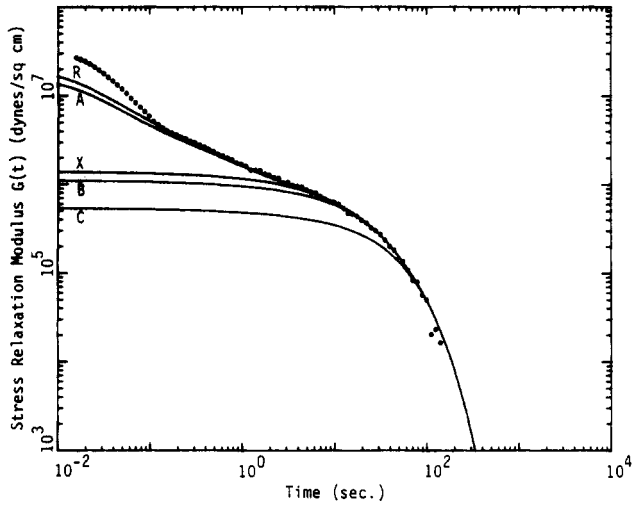

Figure 6. Comparison of the measured (···) and calculated (—) stress relaxation moduli $G(t)$ for the P7/F1 = 75/25 sample. K'/K = 1.88, K''/K = 1, M_e' = 18 000, N_e' = 13, and N_R = 8 are used in the calculation.

$G''(\omega)$ values are compared in Figures 4 and 5, respectively. The separate contributions of the $\mu_R(t)$, $\mu_A(t)$, $\mu_X(t)$, $\mu_B(t)$, and $\mu_C(t)$ processes to $G'(\omega)$ and $G''(\omega)$ are shown in the figures as labeled. The difference between the calculated and measured $G'(\omega)$ values localized in the very high frequency region is due to the glassy relaxation process, which has not been included in eq 1. The effect of the glassy relaxation process on the $G''(\omega)$ values extends to the lower frequency region. The mathematical reason for this has been explained in paper 2. The same effect is observed in all the studied samples as analyzed below.

For P7/F1 = 75/25, the comparison of the calculated and measured $G(t)$ is shown in Figure 6. K'/K = 1.88, K''/K = 1, M_e' = 18 000, and N_e' = 13 are used in the calculation.

For F10/F1 = 50/50, the calculated and measured $G(t)$, $G'(\omega)$, and $G''(\omega)$ values are compared in Figures 7–9, respectively. K'/K = 1.8, K''/K = 1, M_e' = 27 000, and N_e' = 20 are used in the calculations.

For F10/F1 = 75/25, the calculated and measured $G'(\omega)$ and $G''(\omega)$ are compared in Figures 10 and 11, respectively. K'/K = 2.3, K''/K = 1, M_e' = 18 000, and N_e' = 13 are used in the calculation.

For F35/F1 = 50/50, the calculated and measured $G'(\omega)$ and $G''(\omega)$ are compared in Figures 12 and 13, respectively. K'/K = 4.1, K''/K = 1.2, M_e' = 27 000, and N_e' = 20 are

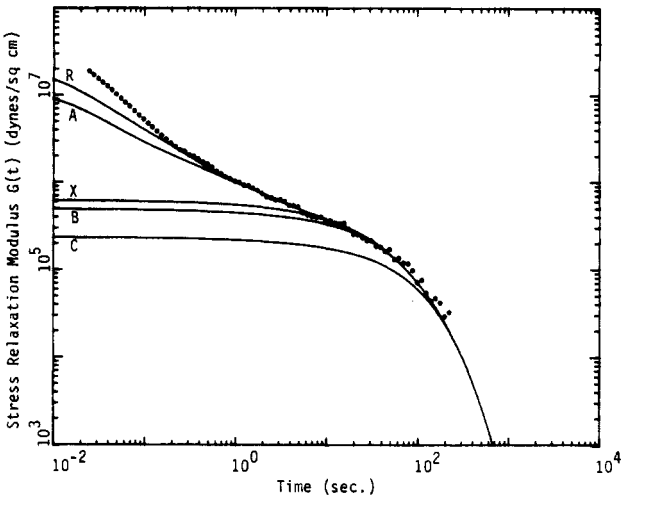

Figure 7. Comparison of the measured (···) and calculated (—) stress relaxation moduli $G(t)$ for the F10/F1 = 50/50 sample. K'/K = 1.8, K''/K = 1, M_e' = 27 000, N_e' = 20, and N_R = 8 are used in the calculation.

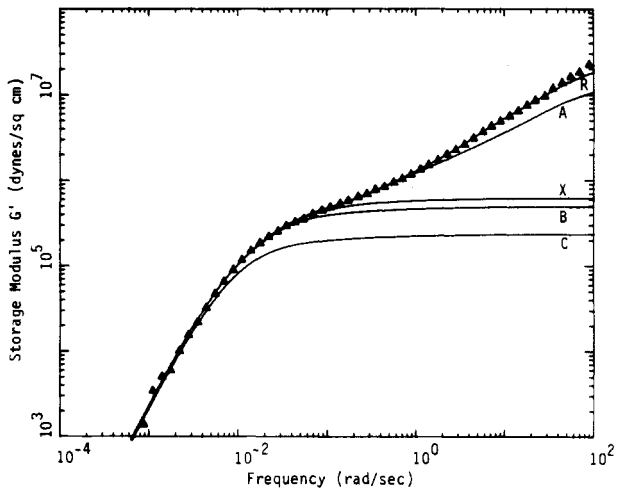

Figure 8. Same as Figure 7 for the storage moduli, $G'(\omega)$, measured (▲) and calculated (—).

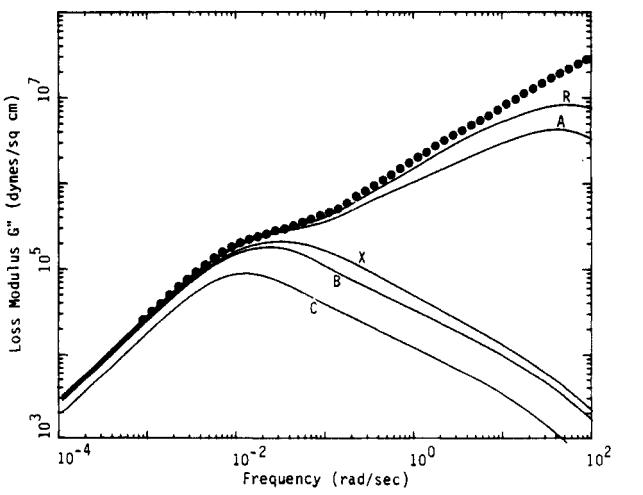

Figure 9. Same as Figure 7 for the loss moduli, $G''(\omega)$, measured (●) and calculated (—).

used in the calculation. The waviness of the calculated $G''(\omega)$ curve in the terminal region is due to the discontinuity nature of the three-component MWD used in the calculation.

For F80/F1 = 50/50, the calculated and measured $G(t)$, $G'(\omega)$, and $G''(\omega)$ values are compared in Figures 14–16,

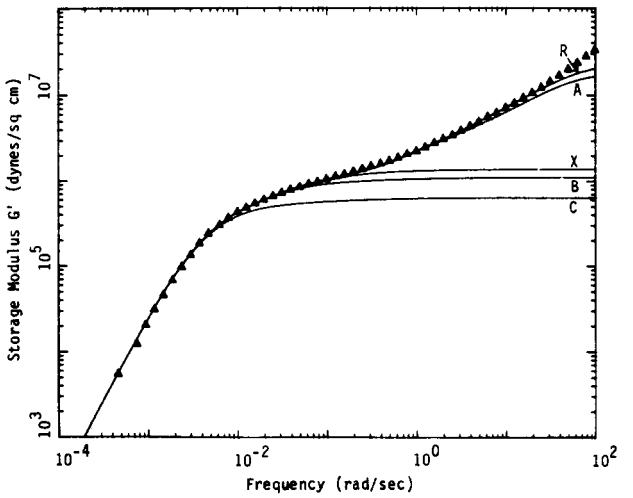

Figure 10. Comparison of the measured (▲) and calculated (—) storage moduli $G'(\omega)$ for the F10/F1 = 75/25 sample. K'/K = 2.3, K''/K = 1, M_e' = 18000, N_e' = 13 and N_R = 8 are used in the calculation.

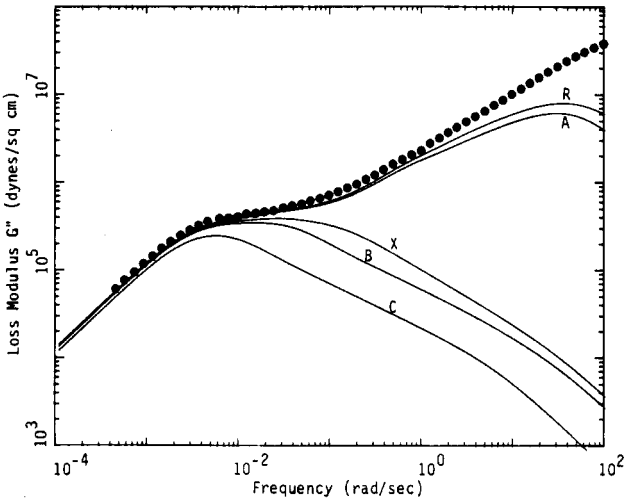

Figure 11. Same as Figure 10 for the loss moduli, $G''(\omega)$, measured (●) and calculated (—).

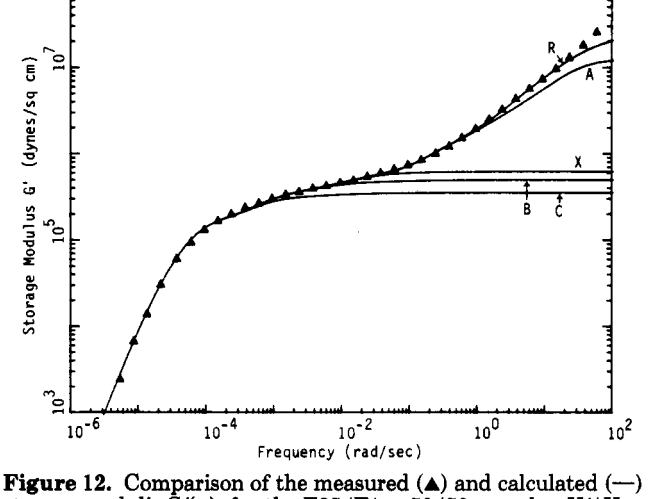

Figure 12. Comparison of the measured (▲) and calculated (—) storage moduli, $G'(\omega)$, for the F35/F1 = 50/50 sample. K'/K = 4.1, K''/K = 1.2, M_e' = 27000, N_e' = 20, and N_R = 8 are used in the calculation.

respectively. K'/K = 4.2, K''/K = 1.3, M_e' = 27000 and N_e' = 20 are used in the calculation. The plateau moduli of the pure F80 and the F80/F1 blend are 5–8% smaller than the corresponding values of the other samples. We

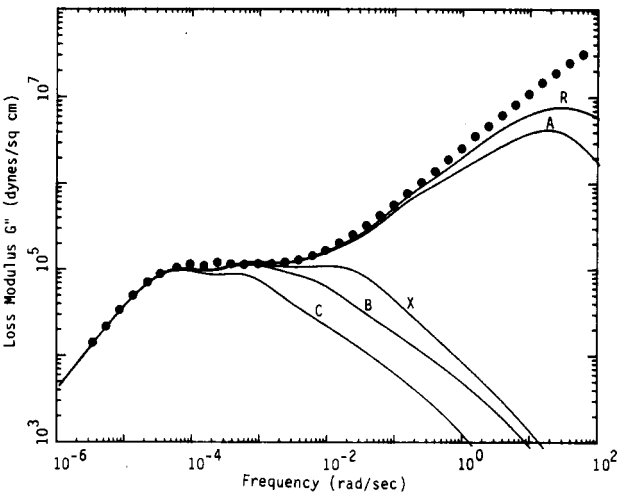

Figure 13. Same as Figure 12 for the loss moduli, $G''(\omega)$, measured (●) and calculated (—).

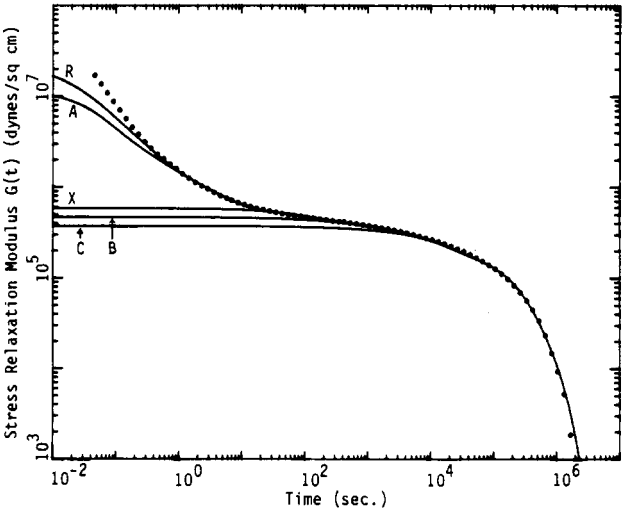

Figure 14. Comparison of the measured (···) and calculated (—) stress relaxation moduli, $G(t)$, for the F80/F1 = 50/50 sample. K'/K = 4.2, K''/K = 1.3, M_e' = 27000, N_e' = 20, and N_R = 8 are used in the calculation.

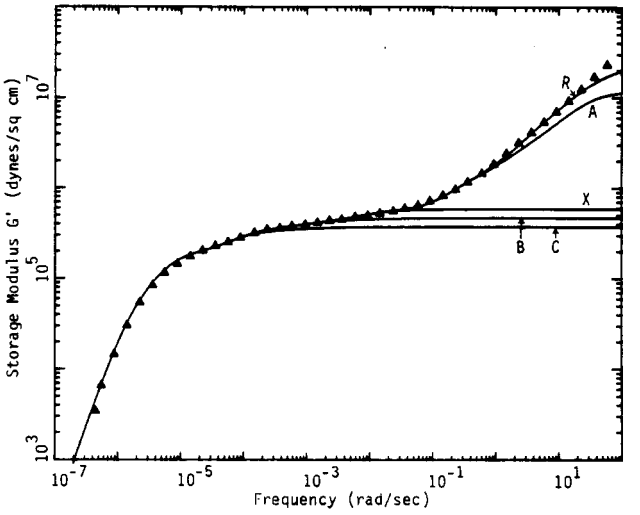

Figure 15. Same as Figure 14 for the storage moduli, $G'(\omega)$, measured (▲) and calculated (—).

believe that the lower G_N value associated with F80 is due to the low-MW components existing in this sample as observable in its GPC spectrum (see paper 1).[1] The measured $G(t)$ and $G'(\omega)$ values in the X process region

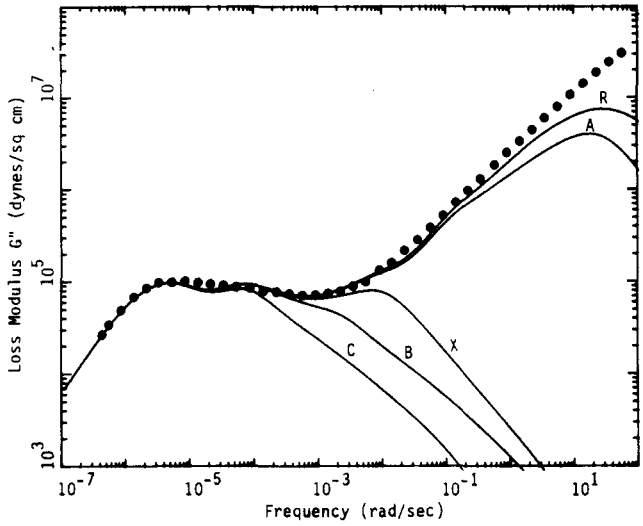

Figure 16. Same as Figure 14 for the loss moduli, $G''(\omega)$, measured (●) and calculated (—).

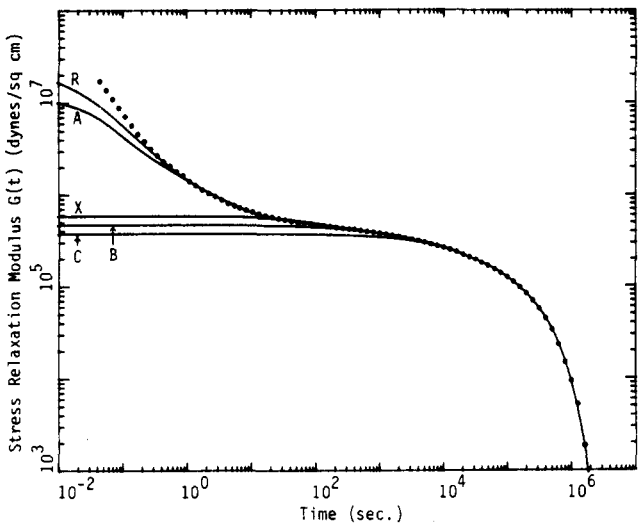

Figure 17. Same as Figure 14. The MWD used in the calculation is, however, obtained directly from analyzing the measured $G(t)$ line shape of the F80/F1 = 50/50 sample. See the text. $K'/K = 4$ and $K''/K = 1.25$ are used in the calculation instead of the values in Figure 14.

being slightly lower than the calculated values may reflect the relaxation of the low-MW components in the sample. In general the low-MW components by the tube-renewal mechanism broaden the MWD that can be extracted from the $G(t)$ line shape analysis. This effect has been explained in paper 2.[8] As a consequence, it has an observable effect on the obtained K'/K and K''/K values, which will be further discussed below.

We have also done nonlinear least-squares fitting directly to the measured $G(t)$ of the F80/F1 = 50/50 sample to extract the three-component MWD of F80. The M_w/M_n value of the obtained MWD is 1.2, which is smaller than that obtained from analyzing the $G(t)$ of the pure F80. For comparison, the theoretical $G(t)$ curve over the entire time domain calculated with this MWD is shown together with the measured values in Figure 17. $K'/K = 4$ and $K''/K = 1.25$ are used in the calculation. They are nearly identical with those used in calculating the $G(t)$ curve shown in Figures 14–16. The reduced MW (M/M_e') of the F80/F1 = 50/50 sample is half that of the pure F80. Thus, the contribution of its $\mu_B(t)$ process to $G(t)$ is greater and its modulus plateau is not as wide.[1,8] This translates into a smaller $\Delta t/\Delta G$ in the plateau region. The obtained

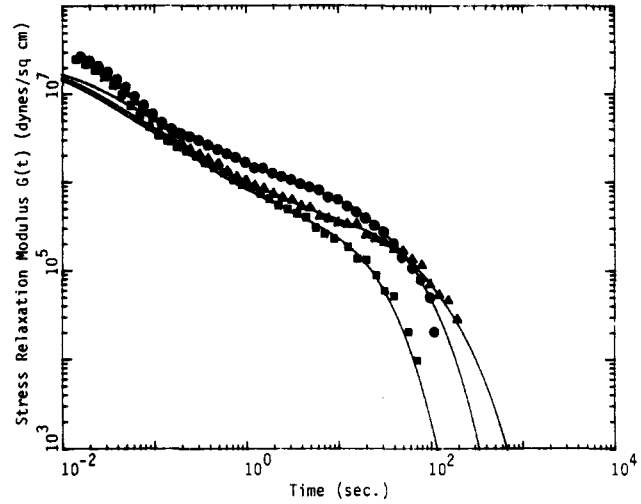

Figure 18. Comparison of the stress relaxation moduli, $G(t)$, (both the calculated (—) and measured) of the P7/F1 = 75/25 (●), P7/F1 = 50/50 (■), and F10/F1 = 50/50 (▲) samples.

M_w/M_n value (1.2) being smaller than that (1.24) extracted from $G(t)$ of the pure F80 is, thus, expected. This supports the conclusion[8] that the $G(t)$ line shape and the MWD that can be extracted from it are sensitive to the low-MW component at high reduced MWs. There is some artificial element in the forced fitting to the $G(t)$ line shape,[8] largely due to the low-MW tail and partly due to the intrinsic broader MWD in the high-MW sample. The obtained values of the parameters K'/K and K''/K have some errors, which are not large and leave the important phenomenon as discussed in the next section still observable.

The line shapes of the linear viscoelastic relaxation spectra of the studied X/F1 blend samples are well described by the general theory. The uniqueness of the theory in describing the line shapes is particularly distinct, when we compare the $G(t)$ line shapes of the P7/F1 = 50/50, P7/F1 = 75/25, and F10/F1 = 50/50 samples as shown in Figure 18.

According to eq 14 (or A2) and 13, the P7/F1 = 50/50 and F10/F1 = 50/50 samples have the same plateau modulus ($G_N' = \rho RT/5M_e$) and entanglement MW ($M_e' = 2M_e$). This is reflected by the similarity between their $G(t)$ line shapes in the time region of the $\mu_R(t)$ and $\mu_A(t)$ processes.

On the other hand, the M/M_e' values of the P7/F1 = 75/25 and F10/F1 = 50/50 samples are about the same (~3.7). According to eq 6–11, the $G(t)$ line shape in the terminal region is strongly related to the M/M_e' value. This is reflected by the closeness of the $G(t)$ line shapes of the two samples in the long-time region, after taking the factor $(M_1/M_2)^2 = 2.2$ (M_1 and M_2 are MW for F10 and P7, respectively) into account. (See eq 11.)

Because of the different combinations of the M_e', M/M_e', and M values, the $G(t)$ line shapes of the three samples compared in Figure 18 show up distinctly different from each other. Each of them is uniquely described by the general theory.

The uniqueness of the general theory in describing the linear viscoelastic relaxation line shapes is further illustrated by the comparison of the calculated and measured $G'(\omega)$ curves of the F10, F10/F1 = 75/25, and F10/F1 = 50/50 samples as shown in Figure 19. With dilution by F1, the plateau modulus decreases according to eq 14 and at the same time the rubbery relaxation and the terminal relaxation are brought closer. This is so because τ_C, τ_B, and τ_X normalized with respect to τ_A[1] are functions of the reduced MW, M/M_e', only. The characteristic line shape

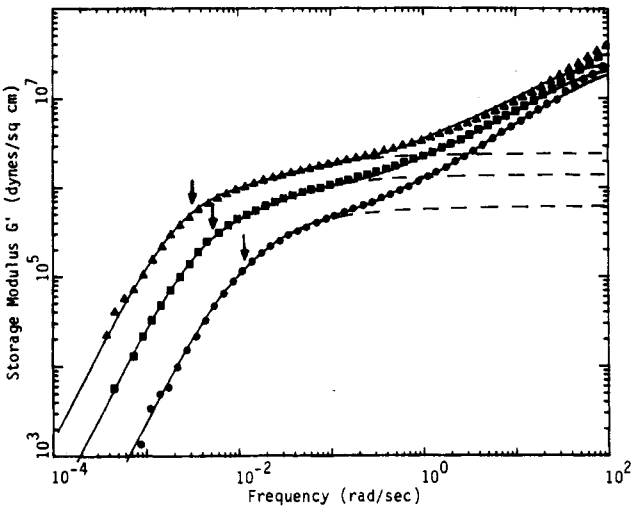

Figure 19. Comparison of the storage moduli, $G'(\omega)$, (both the calculated (—) and measured) of the F10 (▲), F10/F1 = 75/25 (■), and F10/F1 = 50/50 (●) samples. The arrows indicate the frequencies $\omega_C = 1/\tau_C$, where the τ_C values are calculated from eq 11 using $K = 1 \times 10^{-8}$, $M = 100\,000$, and $M_e' = 13\,500\ W_H^{-1}$. The dash lines indicate the separation between the region of $\mu_A(t)$ (and $\mu_R(t)$ for solutions) and the region of $\mu_X(t)$, $\mu_B(t)$, and $\mu_C(t)$.

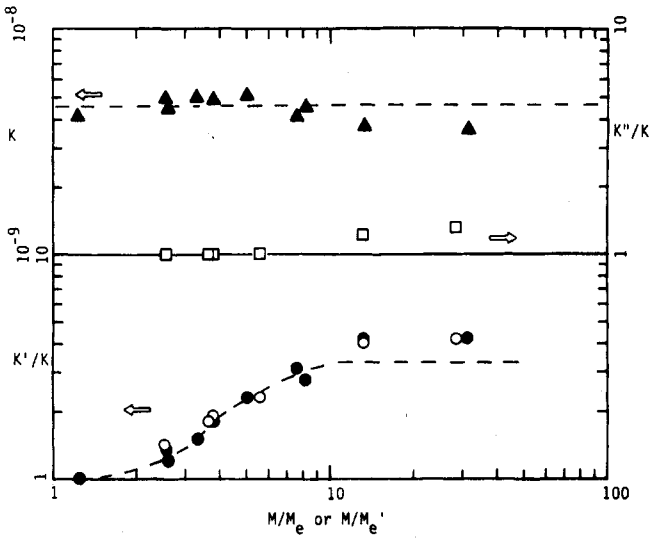

Figure 20. K ((▲) data from paper 2), K''/K ((□) data for the X/F1 blends of the present study) and K'/K ((●) data for the monodisperse melts from paper 2; (○) data for the X/F1 blends of the present study) values as a function of the reduced molecular weight, M/M_e or M/M_e'.

changes with dilution are fully described by the general theory. The only adjustable parameter is the K'/K ratio in describing the changes; the same MWD and $K''/K = 1$ are used in the calculations of the theoretical curves. The obtained K'/K values fall on the universal curve of the pure monodisperse melts as shown below.

V. K Values (Equivalent to the Friction Constants)

From studying a series of monodisperse polystyrene melts, we have observed that K'/K has a plateau value of 3.3 in the high-MW region and decreases to a limiting value of 1 with decreasing MW and that K is independent of MW to as low as $1.2M_e$.[8] It has been proposed that, for $K'/K > 1$, the friction constant for the polymer chain segment to move in the direction perpendicular to the chain contour is higher than that to move along the chain contour. This is a reasonable explanation if we consider that a certain local extra free volume is associated with the polymer chain end. This extra free volume is always available to the $\mu_B(t)$ and $\mu_C(t)$ processes, in which the polymer chain moves along the chain contour. On the other hand, the portion of this extra free volume available to the $\mu_A(t)$ process of a polymer chain depends on the concentration of chain ends of polymer molecules surrounding it. Thus, the K' value extracted from the $\mu_A(t)$ process is MW dependent. Furthermore, the K'/K value approaching 1 at low MW supports this explanation.

As we discussed in detail in paper 3,[9] the anisotropy of the free volume distribution on the polymer chain described above for $K'/K > 1$ begins to appear at $\sim M_e(+)$ like a "phase" transition. Thus, the anisotropic free volume distribution has much to do with the topological constraint of entanglement.

At M_e, the zero-shear viscosity of the Doi–Edwards theory is greater than that of the Rouse theory by a factor of 2.4 (the same K value in both theories). The general linear viscoelastic theory has bridged the gap to ~30% (using $K'/K = 1$ in the calculation with the general theory).[9] The spectrum line shape analyses at the MWs just below and above M_e indicate that the 30% difference should be due to initiation of the topological constraint effect at M_e. In other words, the results of the line shape analysis support that the K values in the general linear viscoelastic theory and in the Rouse theory are identical and the general theory has bridged the gap between the Rouse theory and the Doi–Edwards theory. This cannot be further tested with the relaxation time determinations of monodisperse samples with MW above and below M_e because of the sensitive MW dependence of free volume in this MW region, which affects the K value. However, the X/F1 blends actually provide systems for testing this deduction.

Averaged over the distribution of the component concentrations in the X/F1 blend systems, the free volume distributions on the chain ends of the high-MW chain as well as over the entire Rouse chain of F1 should be statistically identical; *both are free from the topological constraint effect of entanglement.*

In this study, we have found that the obtained K'/K values of the studied X/F1 blend samples fall on the same curve of the K'/K values of the monodisperse polystyrene samples when both sets of data are expressed as a function of the reduced MW (M/M_e' or M/M_e). The results are shown together with the K and K'/K values of the monodisperse components in Figure 20.

We can conclude that the reduced MW dependence of K'/K is universal. This is in agreement with the previous conclusion that the anisotropic free volume distribution associated with $K'/K > 1$ has much to do with the topological constraint effect of entanglement. The result strongly suggests that the topological constraint effect is the sole reason for $K'/K > 1$. The decrease of K'/K with decreasing MW to reach a limiting value of 1 at M/M_e or M/M_e' is caused by the extra free volume associated with the polymer chain ends.[8] The distribution domain size of this extra free volume at chain ends should be larger for the X/F1 blend systems than for the pure monodisperse melts. The characteristic size of the extra free volume distribution domain should be proportional to the M_e or M_e' value, depending on whether the system is a monodisperse melt or a X/F1 blend. The cause for the initiation of the topological constraint effect at M_e is a very fundamental problem. It may be related to the microstructure and the stiffness of the polymer chain of sufficiently short length.

The reduced MW dependence of K''/K is also shown in Figure 20. The sensitivity of the curve fitting in the $\mu_R(t)$

process region to the chosen K''/K value is shown in Figure 3 for the P7/F1 = 50/50 sample as a representative case. In the figure, both the curves calculated with $K''/K = 1$ and 1.5 are compared with the experimental results.

At high MW, the K''/K values tend to be slightly greater than 1. As explained in paper 2 and above, the K values obtained from the $G(t)$ line shape analysis tend to be underestimated at high MWs because of the MWD effect. The amount of underestimation expressed as percentage is about equal to the deviation of the obtained K''/K values from 1. After correcting for this systematic error of the K''/K values, we can conclude from the quality of curve fittings to experimental results shown in Figures 1–17 that $K''/K = 1$ within an experimental error of about 20% for all the studied blend samples. Here, we should also note that only one "solvent" polymer is used. Since the requirement of the sample characterization is very crucial in the actual line shape analysis, we think, under the circumstance of lacking well-characterized samples in this low-MW range, that a very well-characterized sample is better than several samples of less quality. We believe that the F1 sample used here is very well characterized. For $K''/K = 1$, the error that can be caused by any uncertainty of the F1 sample should be well within the possible experimental error quoted above.

In the X/F1 blend samples, the K value should decrease with increasing amount of F1 component, because F1 has more free volume. Correspondingly, the K'' value of the F1 component (the K value of the Rouse component) is increased by the presence of the high-MW component. The observed result that $K''/K = 1$ in the X/F1 blend systems is in agreement with the observation that K'/K reaches a limiting value of 1, when M approaches M_e, and strongly supports the conclusion that the general linear viscoelastic theory has bridged the gap between the Doi–Edwards theory and the Rouse theory.

VI. Implication in the Blending Law

In this study of polymer blends consisting of two monodisperse polystyrene components, of which one has MW below M_e, eq 13 is well followed. Two observations support this: (1) The plateau modulus, G_N', of the solution as a function of concentration is in good agreement with eq 14. The agreement is within ±5% for all the samples studied, while virtually perfect for most of the low-MW samples. (2) The measured $G(t)$ line shapes are well described by eq 1 in combination with eq 2–11 and 15. In the comparison of theory and experiment, the *same* MWDs obtained from the line shape analysis of linear viscoelastic relaxation spectra of the monodisperse melts and M_e' as given by eq 13 are used in the calculation. These results also strongly support that the universality of the general linear viscoelastic theory is as much applied to the concentrated solution systems as to the monodisperse melts.

The entanglement MW is increased by dilution. Correspondingly, the entanglement distance or the tube size (of the Doi–Edwards theory) is enlarged. As a result, the relaxation time τ_C as given by eq 11 is shortened by dilution, even if the friction constant or the K value did not change with increase of free volume. The normalized relaxation time τ_C/τ_A^1 becomes even smaller, because of the $M_e'^2$ dependence of τ_A^1. This is well demonstrated by the example shown in Figure 19.

For understanding the molecular mechanism for the blend law that covers a wide MW range, we consider the binary blend system, in which both MW components are above M_e. The basic theoretical form for $G(t)$ of such a binary blend is given in the Appendix and in ref 21 of paper 2.[8] If the MW of the low-MW component is so close to the M_e value that $T(t)$ (see eq A1) decays to zero in a time much shorter than τ_{CH} (see eq 11), the low-MW component will serve as a solvent (similar to F1) to the high-MW component in the long-time region ($t > \tau_T$) and the entanglement MW for the high-MW component should be given by eq 13. In another extreme, when the low-MW component converges into the high-MW component (equivalent to a monodisperse system consisting of the high-MW component only), the tube-renewal effect that could be caused by the low-MW component disappears. This has been concluded in the study of the monodisperse systems as reported previously.[1,8,9] In between, the entanglement MW at a certain W_H value (denoted as M_e'') should have a value between M_e and M_e' and decrease gradually to M_e with increasing MW of the low-MW component. M_e'' being larger than M_e should have effect on the relaxation time, τ_{CH}, in the terminal region. Phenomenologically, we have observed the shortening of the longest relaxation time. On the other hand, τ_{BH} is independent of entanglement MW according to eq 9. For polystyrene, we have observed that the concentration dependence of the plateau modulus of the high-MW component in a binary blend with both components having MWs higher than M_e is well described by that given in eq A1 (i.e., the plateau modulus after the completion of the $T(t)$ relaxation, which is identical with eq 14). The results will be presented in a future report.

For some other kinds of polymers (such as polyisoprene), a slightly stronger concentration dependence of the plateau modulus ($G_N \propto W_H^X$, $X = 2.1$–2.2) has been observed.[12,13] There is no explanation for it at the present time. This discrepancy may be related to the microstructure of the polymer rather than to the topological constraint of entanglement as described here.

VII. Conclusion

In this study, we have shown the validity and universality of the proposed general linear viscoelastic theory as applied to the concentrated solution systems, in which the solvent is a low-MW homopolymer. The consistency of the MWDs used in the theoretical calculations is preserved between the melt and solution cases. This is very significant, because the universality and applicability of the proposed general theory is shown extending beyond explaining the well-known 3.4 power law of the zero-shear viscosity and the $G(t)$ line shapes of monodisperse melts.

The K values in the Rouse theory and the proposed general linear viscoelastic theory are shown identical within experimental error. In other words, the results strongly support that the proposed general theory has bridged the gap between the Rouse theory and the Doi–Edwards theory.

We have extracted the K'/K values from the line shape analysis of the linear viscoelastic relaxation spectra in terms of the proposed general theory. The results $K'/K > 1$ at MWs greater than M_e strongly indicate that the friction constant for the polymer segment to move in the direction perpendicular to the chain contour is greater than that to move along the chain contour. When MW is normalized with respect to M_e or M_e', the reduced MW dependence of K'/K is universal for both the monodisperse melts studied previously and the concentrated solution systems of the present study. We have concluded that $K'/K > 1$ is due to the topological constraint effect of entanglement and that the decrease of K'/K with decreasing MW to reach a limiting value of 1 at M/M_e or $M/M_e' \sim 1$ is caused by the extra free volume associated with the polymer chain ends. We believe that this is a very significant phenomenon and has been discovered only

because the proposed general theory can successfully describe the linear viscoelastic relaxation spectra of the studied melt and concentrated solution samples.

The proposed general linear viscoelastic theory for monodisperse polymers provides a basis for studying blend systems consisting of two monodisperse components whose MWs are both higher than M_e. The present study indicates that the tube size should enlarge gradually with decreasing M_L to a limiting value as given by eq 13 at a fixed W_H value. This effect should be reflected in the variation of τ_{CH} with M_L.

To put the presently reported study in perspective, it is appropriate to mention here some preliminary observations at a lower concentration, X/F1 = 25/75, as a final note. At this low concentration, the line shapes of the viscoelastic spectra deviate from the proposed general linear viscoelastic theory. The deviation appears related to a too small K value, which can be caused by a tube–renewal process at sufficient low concentrations. A recent study[17] as to the reason why the tube renewal process is negligible for the viscoelastic properties of a nearly monodisperse melt does suggest that the tube–renewal process can become important when the concentration of the polymer solution is sufficiently low yet still in the entanglement regime. Further, X/F1 = 25/75 appears close to the concentration region, where the polymer solutions transit from the concentrated regime to the semidilute regime. It has been suggested that the transition concentration is independent of MW and is around 0.05–0.2 g/mL.[18] At X/F1 = 25/75, the solutions may already be influenced by the good solvent property (the excluded volume effect) that can occur in the semidilute regime. It is hard to judge now whether the two effects described above, tube-renewal process and excluded volume effect, are related in a meaningful way. In any case, the deviation at X/F1 = 25/75 may very well be expected, since the proposed general linear viscoelastic theory is supposed to hold only in melts and concentrated solutions.

Appendix

The blending law can be basically described by the following stress relaxation function for a blend system consisting of two monodisperse components whose MWs are both greater than M_e and far apart from each other (without including the A and X processes) (see ref 21 of paper 2)

$$G(t) = \left(\frac{4\rho RT}{5M_e}\right) W_L[B_L\mu_B(t/\tau_{BL}) + C_L\mu_C(t/\tau_{CL})] + \left(\frac{4\rho RT}{5M_e}\right) W_H[W_L T(t) + W_H][B_H\mu_B(t/\tau_{BH}) + C_H\mu_C(t/\tau_{CH})] \quad \text{(A1)}$$

where $T(t)$ is a decaying function for the tube-renewal process with a characteristic time τ_T, which is experimentally larger than the τ_{CL} value by about a factor of 7. The $T(t)$ process is caused by the disentanglement of the low-MW chains from the high-MW chains. Consider the case where the low-MW component has a MW (M_L) below M_e. Because it experiences no entanglement, the molecular dynamics of the low-MW component is best described by the Rouse theory and $T(t)$ decays to zero very quickly. For this case, eq A1 can be rewritten as

$$G(t) = W_L \frac{\rho RT}{M_L}\mu_R(t/\tau_R) + \frac{4\rho RT}{5(M_e/W_H)} W_H[B_H\mu_B(t/\tau_{BH}) + C_H\mu_C(t/\tau_{CH})] \quad \text{(A2)}$$

The prefactor of the second term says that the entanglement MW is increased to a value, $M_e' = M_e W_H^{-1}$ by dilution.

When the A and X processes of the high-MW component are included, eq 1 is obtained (with the subscript H omitted). Because entanglement MW is increased to $M_e' = M_e W_H^{-1}$ by dilution, the M_e quantity that appears in all the relaxation times (τ_A, τ_X, and τ_C) and the relaxation strengths (B and C) of the monodisperse system need be replaced by M_e' for the present blend (or concentrated solution) systems.

The present argument for obtaining $M_e' = M_e W_H^{-1}$ is somewhat similar to that based on a simple counting of intermolecular random contacts of a polymer solution.[14,15] The relation, $M_e' = M_e W_H^{-1}$, is in agreement with $a \propto W_H^{-1/2}$ (where a is the entanglement step length) obtained from computer simulations.[16]

Registry No. Polystyrene, 9003-53-6.

References and Notes

(1) Lin, Y.-H. *Macromolecules* **1984**, *17*, 2846.
(2) Doi, M.; Edwards, S. F. *J. Chem. Soc., Faraday Trans. 2* **1978**, *74*, 1789.
(3) Doi, M.; Edwards, S. F. *J. Chem. Soc., Faraday Trans. 2* **1978**, *74*, 1802.
(4) Doi, M.; Edwards, S. F. *J. Chem. Soc., Faraday Trans. 2* **1978**, *74*, 1818.
(5) Doi, M.; Edwards, S. F. *J. Chem. Soc., Faraday Trans. 2* **1979**, *75*, 38.
(6) Doi, M. *J. Polym. Sci., Polym. Lett. Ed.* **1981**, *19*, 265.
(7) Doi, M. *J. Polym. Sci., Polym. Phys. Ed.* **1983**, *21*, 667.
(8) Lin, Y.-H. *Macromolecules* **1986**, *19*, 159.
(9) Lin, Y.-H. *Macromolecules* **1986**, *19*, 168.
(10) Lin, Y.-H. *Macromolecules* **1985**, *18*, 2779. In a recent publication (*Macromolecules*, **1986**, *19*, 1108), Kramer et al. corrected the temperature at which the diffusion motion data were measured from 170 to 174 °C. With adjustment to their new temperature, the average ratio of the *pure* reptation times calculated from my linear viscoelastic data (τ_C^0) and their diffusion motion data (T_d) becomes $T_d/\tau_C^0 = 1.85$ (vs. 1.27 at 170 °C). In paper 2 (ref 8), it has been shown that the K value (proportional to τ_C^0) obtained from the $G(t)$ line shape analysis *in the high MW region* (also see ref 1) is smaller than what it should be by about 30% due to the MWD of the sample. After corrections are made for this MWD effect, $T_d/\tau_C^0 = 1.3$. Considering the possible errors from different sources, this agreement between T_d and τ_C^0 is very good.
(11) de Gennes, P.-G. *Scaling Concepts in Polymer Physics*; Cornell University Press: Ithaca, NY, and London, 1979; p 60.
(12) Graessley, W. W.; Edwards, S. F. *Polymer* **1981**, *22*, 1329.
(13) Lin, Y.-H., unpublished results.
(14) Graessley, W. W. *Adv. Polym. Sci.* **1974**, *16*, 1.
(15) Graessley, W. W. *Faraday Symp. Chem. Soc.* **1983**, *18*, 1.
(16) Evans, K. E.; Edwards, S. F. *J. Chem. Soc., Faraday Trans 2* **1981**, *77*, 1891, 1913, 1929.
(17) Lin, Y.-H. *Macromolecules*, submitted.
(18) Graessley, W. W. *Polymer* **1980**, *21*, 258.